

Properties of 125 GeV Higgs boson in non-decoupling MSSM scenarios

Kaoru Hagiwara,^a Jae Sik Lee,^b Junya Nakamura^a

^a*KEK Theory Center and Sokendai, Tsukuba, Ibaraki 305-0801, JAPAN*

^b*Department of Physics, National Tsing Hua University, Hsinchu, Taiwan 300*

E-mail: kaoru.hagiwara@kek.jp, jslee@phys.nthu.edu.tw,
junnaka@post.kek.jp

ABSTRACT: Tantalizing hints of the Higgs boson of mass around 125 GeV have been reported at the LHC. We explore the MSSM parameter space in which the 125 GeV state is identified as the heavier of the CP even Higgs bosons, and study two scenarios where the two-photon rate can be significantly larger than the standard model. In one scenario, $\Gamma(H \rightarrow \gamma\gamma)$ is enhanced by a light stau contribution, while the WW^* (ZZ^*) rate is not, or slightly smaller than the SM rate. In the other scenario, $\Gamma(H \rightarrow b\bar{b})$ is suppressed and not only the $\gamma\gamma$ but also the WW^* (ZZ^*) rates should be enhanced. The $\tau\bar{\tau}$ rate can significantly be larger than the SM rate in both scenarios. Other common features of the scenarios include top decays into charged Higgs boson, single and pair production of all neutral Higgs bosons in e^+e^- collisions at $\sqrt{s} \lesssim 400$ GeV.

KEYWORDS: Higgs boson, MSSM

Contents

1	Introduction	1
2	Higgs sector in MSSM	2
3	Scenarios giving large two photon rates	4
3.1	Light stau scenario	7
3.1.1	$R_{\gamma\gamma}$	7
3.1.2	R_{ZZ}	9
3.1.3	$R_{\tau\bar{\tau}}$	9
3.2	Small $\Gamma(H \rightarrow b\bar{b})$ scenario	11
3.2.1	$R_{\gamma\gamma}$ and R_{ZZ}	11
3.2.2	$R_{\tau\bar{\tau}}$	12
4	Constraints on the other Higgs bosons	13
5	Conclusion	14

1 Introduction

Latest results from the Higgs boson search by the ATLAS [1] and the CMS [2] collaborations show an excess of events around the mass region of 125 GeV. The main search channel is the two photons decay mode of the Higgs boson, for which both experiments reported the rate higher than the standard model (SM) prediction. There are hints of the ZZ^* decay mode with less significance, while no hints have been reported for the $\tau\bar{\tau}$ mode. We expect that the data from the current 8 TeV run will make clear the properties of the Higgs boson candidate.

The Higgs sector in the minimal supersymmetric standard model (MSSM) has five physical mass eigenstates, two CP even and one CP odd neutral scalar bosons, if CP is conserved in the Higgs sector, and one pair of charged scalar bosons [3]. The observed $\gamma\gamma$ resonance at 125 GeV can be one of the three neutral Higgs bosons. Among them, the CP odd state (A) cannot give the $\gamma\gamma$ rate greater than that of the SM Higgs bosons, mainly it lacks the W boson loop contribution to the $\gamma\gamma$ decay [4]. Among the two CP even Higgs bosons, both the light mass eigenstate (h) and the heavier one (H) can be 125 GeV and can have enhanced $\gamma\gamma$ rate. MSSM scenarios where the lighter of the CP even Higgs boson is identified as the 125 GeV state are discussed in refs.[5–19], and the possibility of the 125 GeV state as the heavier of the CP even Higgs bosons is discussed in ref.[16]. The former scenario contains the so-called decoupling region where all the other Higgs bosons (H , A , H^\pm) are significantly heavier than the lighter CP even state h , whose properties resembles

the SM one. On the other hand, in the latter scenario where the heavier of the CP even state H has the mass 125 GeV, not only the mass of the lighter CP even state h but also those of the CP odd state A and the charged Higgs boson H^\pm are bounded from above.

In this study, we study carefully the consequences of this non-decoupling scenario of MSSM where the 125 GeV state is the heavier of the CP even Higgs bosons, H . In particular, we study two sub-scenarios where the two photon production rate can be larger than the SM. In scenario 1, the partial width $\Gamma(H \rightarrow \gamma\gamma)$ is enhanced by a light stau loop contribution while the WW^* (ZZ^*) rate is slightly smaller than the SM rate. In scenario 2, the dominant partial width $\Gamma(H \rightarrow b\bar{b})$ is suppressed and not only $\gamma\gamma$ but also WW^* (ZZ^*) production rate can be large. In both scenarios, the $\tau\bar{\tau}$ rate can be significantly larger than the SM. Predictions for the mass spectrum of the other Higgs bosons are also examined.

The enhancement of the two photon production rate due to a light stau in the decoupling region has been studied in refs.[12, 19]. We show in this report that the same mechanism works for the non-decoupling region as well. The suppression of $\Gamma(H \rightarrow b\bar{b})$ in the non-decoupling region has been studied in [16]. We study not only the $\gamma\gamma$ and ZZ^* rates but also the $\tau\bar{\tau}$ rate in detail.

2 Higgs sector in MSSM

In this section, we review briefly the mass spectrum of the Higgs bosons in MSSM. In our scenarios where the two photon production rate of the heavier CP even state H is higher than the SM, relatively large Higgs couplings to the weak bosons are necessary, since the main contribution to the $H \rightarrow \gamma\gamma$ transition comes from the W boson loop [4]. Hence, H must be a SM-like Higgs boson.

The MSSM Higgs sector consists of two $SU(2)_L$ doublets, ϕ_u and ϕ_d which give masses to up type fermions and down type fermions, respectively [3]. When the electroweak symmetry is spontaneously broken, MSSM gives five physical mass eigenstates, two CP even scalar bosons h and H , one CP odd scalar boson A , and one pair of charged scalar bosons H^\pm . The two CP even scalar bosons are mixed states of the real components of the two Higgs doublets,

$$\begin{pmatrix} h \\ H \end{pmatrix} = \begin{pmatrix} \cos \alpha & -\sin \alpha \\ \sin \alpha & \cos \alpha \end{pmatrix} \begin{pmatrix} H_u^0 \\ H_d^0 \end{pmatrix}, \quad (2.1)$$

where we define h and H as the lighter and the heavier of the two CP even scalar bosons, respectively, whereas the current basis states H_u^0 and H_d^0 are defined as

$$\text{Re}(\phi_u^0) = \frac{v_u + H_u^0}{\sqrt{2}}, \quad \text{Re}(\phi_d^0) = \frac{v_d + H_d^0}{\sqrt{2}}. \quad (2.2)$$

Considering the convention that vacuum expectation values of the two Higgs doublets are written as $v_u = v \sin \beta$ and $v_d = v \cos \beta$ where v ($\simeq 245$) GeV is the vacuum expectation

value of the SM Higgs doublet, we can introduce another base

$$\begin{pmatrix} H_u^0 \\ H_d^0 \end{pmatrix} = \begin{pmatrix} \sin \beta & -\cos \beta \\ \cos \beta & \sin \beta \end{pmatrix} \begin{pmatrix} H_{SM} \\ H_\perp \end{pmatrix}, \quad (2.3)$$

where H_{SM} is the state whose couplings to all the SM particles are the same as those of the SM Higgs boson, and H_\perp is its orthogonal state which has no coupling to weak bosons. From eqs.(2.1, 2.3), we have

$$h = -\sin(\alpha - \beta)H_{SM} - \cos(\alpha - \beta)H_\perp, \quad (2.4a)$$

$$H = \cos(\alpha - \beta)H_{SM} - \sin(\alpha - \beta)H_\perp. \quad (2.4b)$$

Hence, when H is a SM-like Higgs boson and $\tan \beta \gg 1$,

$$\begin{aligned} |\sin \alpha| &\rightarrow 1, \\ |\cos \alpha| &\rightarrow 0, \end{aligned} \quad (2.5)$$

and hence $\cos 2\alpha < 0$ holds. The masses and the eigenstates of the CP even Higgs bosons are determined by diagonalizing the symmetric mass-squared matrix in the space of $(H_u^0, H_d^0)^T$,

$$\begin{pmatrix} M_{uu}^2 & M_{ud}^2 \\ M_{ud}^2 & M_{dd}^2 \end{pmatrix}, \quad (2.6)$$

whose elements can be approximated as [20]

$$M_{uu}^2 \sim M_z^2 \left(1 - \frac{3}{8\pi^2} Y_t^2 \ln \frac{M_{susy}^2}{M_t^2} \right) + \frac{3v^2}{8\pi^2} Y_t^4 \left[\ln \frac{M_{susy}^2}{M_t^2} + \bar{A}_t^2 \left(1 - \frac{\bar{A}_t^2}{12} \right) \right], \quad (2.7a)$$

$$M_{dd}^2 \sim M_A^2 - \frac{v^2}{32\pi^2} Y_t^4 \bar{\mu}^2 \bar{A}_t^2 - \frac{v^2}{32\pi^2} Y_b^4 \bar{\mu}^2 \bar{A}_b^2, \quad (2.7b)$$

$$\begin{aligned} M_{ud}^2 \sim & -\cos \beta \left[M_A^2 + M_z^2 + \frac{v^2}{16\pi^2} Y_t^4 \bar{\mu}^2 (\bar{A}_t^2 - 3) + \frac{v^2}{16\pi^2} Y_b^4 \bar{\mu}^2 (\bar{A}_b^2 - 3) \right] \\ & + \frac{v^2}{32\pi^2} Y_t^4 \bar{\mu} \bar{A}_t (\bar{A}_t^2 - 6) + \frac{v^2}{32\pi^2} Y_b^4 \bar{\mu}^3 \bar{A}_b, \end{aligned} \quad (2.7c)$$

where only the leading terms for large $\tan \beta$ ($\tan \beta \gg 1$) are kept, Y_t and Y_b are, respectively, the top and bottom Yukawa couplings in the MSSM. The soft SUSY breaking A_f terms and the Higgsino mass μ are made dimensionless as $\bar{A}_t = A_t/M_{susy}$, $\bar{A}_b = A_b/M_{susy}$, $\bar{\mu}_t = \mu/M_{susy}$ with

$$M_{susy}^2 = \frac{M_{\tilde{t}_1}^2 + M_{\tilde{t}_2}^2}{2}, \quad (2.8)$$

where $M_{\tilde{t}_1}$ and $M_{\tilde{t}_2}$ are the masses of the stop mass eigenstates. Full analytic formulae of the mass matrix elements can be found in ref.[20]. By diagonalizing the matrix eq.(2.6), we obtain the masses of the two CP even Higgs bosons,

$$M_h^2 = M_{uu}^2 \cos^2 \alpha + M_{dd}^2 \sin^2 \alpha - M_{ud}^2 \sin 2\alpha, \quad (2.9a)$$

$$M_H^2 = M_{uu}^2 \sin^2 \alpha + M_{dd}^2 \cos^2 \alpha + M_{ud}^2 \sin 2\alpha, \quad (2.9b)$$

with

$$\tan 2\alpha = \frac{-2M_{ud}^2}{M_{uu}^2 - M_{dd}^2}. \quad (2.10)$$

In the limit of eq.(2.5), where the state H has the SM-like couplings to the weak bosons, the mass eigenstates in eq.(2.9) become

$$M_h^2 \simeq M_{dd}^2 - 2M_{ud}^2 \cos \alpha + O(\cos^2 \alpha), \quad (2.11a)$$

$$M_H^2 \simeq M_{uu}^2 + 2M_{ud}^2 \cos \alpha + O(\cos^2 \alpha). \quad (2.11b)$$

The condition that the SM-like state H is heavier than the other state reads

$$M_H^2 - M_h^2 = M_{uu}^2 - M_{dd}^2 + 4M_{ud}^2 \cos \alpha + O(\cos^2 \alpha) > 0. \quad (2.12)$$

We note that in the limit of $|\cos \alpha| \rightarrow 0$, eq.(2.5), the above inequality (2.12) implies

$$M_{uu}^2 - M_{dd}^2 > 0, \quad (2.13)$$

or

$$\begin{aligned} M_Z^2 + \frac{3}{8\pi^2} Y_t^2 \ln \frac{M_{susy}^2}{M_t^2} (v^2 Y_t^2 - M_z^2) \\ + \frac{3}{8\pi^2} v^2 Y_t^4 \bar{A}_t^2 \left(1 - \frac{\bar{A}_t^2 - \bar{\mu}^2}{12} \right) + \frac{1}{32\pi^2} v^2 Y_b^4 \bar{\mu}^2 \bar{A}_b^2 \gtrsim M_A^2. \end{aligned} \quad (2.14)$$

Hence M_A is bounded from above by the loop contribution to the Higgs potential. We also note that the $M_{ud}^2 \cos \alpha$ term can be relevant in the inequality eq.(2.12) when

$$M_{ud}^2 \cos \alpha > 0, \quad (2.15)$$

which happens in two separate regions of the MSSM parameter space,

$$(I) \quad M_{ud}^2 < 0 \text{ and } \cos \alpha < 0 \quad \left(\frac{\pi}{2} < \alpha < \frac{3}{4}\pi \right) \quad (2.16a)$$

$$(II) \quad M_{ud}^2 > 0 \text{ and } \cos \alpha > 0 \quad \left(\frac{\pi}{4} < \alpha < \frac{\pi}{2} \right), \quad (2.16b)$$

where the constraints in the mixing angle α in the parentheses follow from $\cos 2\alpha < 0$. The case (II) takes place if the loop contribution in eq.(2.8) dominates over the negative contribution when $\bar{A}_t^2 > 6$. It should also be noted from eqs.(2.7a, 2.11b) that in order to make H as heavy as 125 GeV, large M_{susy} and $\bar{A}_t \sim \sqrt{6}$ are necessary, and we explore the MSSM parameter region which satisfies conditions in the following sections.

3 Scenarios giving large two photon rates

In our analysis, we consider the following Higgs production processes at the LHC,

$$\text{Gluon fusion } gg \rightarrow \phi + X, \quad (3.1a)$$

$$\text{Weak boson fusion } qq \rightarrow qq\phi + X, \quad (3.1b)$$

$$\text{Bottom quark annihilation } b\bar{b} \rightarrow \phi + X, \quad (3.1c)$$

where ϕ can be h, H or A . The MSSM Higgs cross sections are obtained by scaling the corresponding SM Higgs cross sections with the ratio of the MSSM decay width over the SM decay width for the gluon fusion and the b-quark annihilation processes, and with the ratio of the weak boson coupling squared for the weak boson fusion processes. The SM Higgs production cross sections for the above processes in eq.(3.1) are calculated by using the program HIGLU [21], HAWK [22] and BBH@NNLO [23], respectively. The MSSM decay widths, couplings and mass spectrum of the Higgs bosons and SUSY particles are calculated with a updated version of CPsuperH2.0 [24] which includes the stau contributions to the Higgs boson masses. The SM decay widths are calculated with the program HDECAY[25]. Although the SM cross section of b-quark annihilation process is quite small compared to the most dominant gluon fusion process, it may be important in some MSSM scenarios.

We consider the following constraints from the collider experiments. For the stau and stop masses, we adopt the lower mass bounds [26]

$$\text{Stau } M_{\tilde{\tau}} > 81.9 \text{ GeV}, \quad (3.2a)$$

$$\text{Stop } M_{\tilde{t}} > 92.6 \text{ GeV}. \quad (3.2b)$$

Upper bounds on the e^+e^- annihilation cross sections

$$\sigma(e^+e^- \rightarrow Zh(\rightarrow Zb\bar{b} \text{ and } Z\tau\bar{\tau})), \quad (3.2c)$$

$$\sigma(e^+e^- \rightarrow Ah(\rightarrow b\bar{b}b\bar{b}, \bar{b}\bar{b}\tau\bar{\tau} \text{ and } \tau\bar{\tau}\tau\bar{\tau})) \quad (3.2d)$$

are taken from ref.[27], and these on the cross section at the LHC

$$\sigma(pp \rightarrow h, A, H(\rightarrow \tau\bar{\tau})) \quad (3.2e)$$

is taken from ref.[28]. Bound on the branching fraction

$$B(t \rightarrow bH^+(\rightarrow b\bar{\tau}\nu_{\tau})) \quad (3.2f)$$

is taken from ref.[29]. Since all the physical Higgs bosons are relatively light in our non-decoupling scenario when $M_h < M_H \approx 125$ GeV, and all the above constraints on quantities in eqs.(3.2) are required to be satisfied in all the results presented bellow. In particular, significant portion of very large $\tan\beta$ regions is excluded by the $h, A, H \rightarrow \tau\bar{\tau}$ and $t \rightarrow bH^+(\rightarrow \bar{\tau}\nu_{\tau})$ search limits [28, 29].

We define the ratio of the production rate at the LHC as

$$R_{AB} = \frac{\sigma(pp \rightarrow H)B(H \rightarrow AB)}{\sigma(pp \rightarrow H)^{SM}B(H \rightarrow AB)^{SM}}, \quad (3.3)$$

which gives the $H \rightarrow AB$ production rate as compared to the SM prediction. Although we calculate the Higgs boson cross section $\sigma(pp \rightarrow H + X)$ at $\sqrt{s} = 7$ TeV, the ratio R_{AB} should not change significantly even for $\sqrt{s} = 8$ TeV, since the dominance of the gluon fusion process would not change. Hence, our results can also be applied for future results of $\sqrt{s} = 8$ TeV. Since the gluon fusion production process dominates over the other processes, and since the total decay width is dominated by $\Gamma(H \rightarrow b\bar{b})$ for the SM Higgs boson as well

as the heavy CP even state H with mass around 125 GeV in our non-decoupling MSSM scenarios, R_{AB} may be approximately written by using the partial decay widths,

$$R_{AB} \simeq \left(\frac{\Gamma(H \rightarrow gg)}{\Gamma(H \rightarrow gg)^{SM}} \right) \cdot \left(\frac{\Gamma(H \rightarrow b\bar{b})}{\Gamma(H \rightarrow b\bar{b})^{SM}} \right)^{-1} \cdot \left(\frac{\Gamma(H \rightarrow AB)}{\Gamma(H \rightarrow AB)^{SM}} \right). \quad (3.4)$$

By introducing a short hand

$$r_{ab} = \frac{\Gamma(H \rightarrow ab)}{\Gamma(H \rightarrow ab)^{SM}}, \quad (3.5)$$

for a partial width normalized by the corresponding SM value, the production rate R_{AB} of eq.(3.4) can be expressed as

$$R_{AB} \simeq r_{gg} \cdot (r_{b\bar{b}})^{-1} \cdot r_{AB}. \quad (3.6)$$

In this study, we examine $R_{\gamma\gamma}$, R_{ZZ} and $R_{\tau\bar{\tau}}$,

$$R_{\gamma\gamma} \simeq r_{gg} \cdot (r_{b\bar{b}})^{-1} \cdot r_{\gamma\gamma}, \quad (3.7a)$$

$$R_{ZZ} \simeq r_{gg} \cdot (r_{b\bar{b}})^{-1} \cdot r_{ZZ}, \quad (3.7b)$$

$$R_{\tau\bar{\tau}} \simeq r_{gg} \cdot (r_{b\bar{b}})^{-1} \cdot r_{\tau\bar{\tau}}, \quad (3.7c)$$

and identify two scenarios where the following two conditions are satisfied for the heavier CP even Higgs boson in the MSSM,

$$123 < M_H < 127 \text{ GeV} \quad (3.8a)$$

$$1 < R_{\gamma\gamma} < 3. \quad (3.8b)$$

They are

$$\text{Light stau scenario : } r_{\gamma\gamma} > 1 \text{ and } r_{gg} \cdot (r_{b\bar{b}})^{-1} \sim 1 \quad (3.9a)$$

$$\text{Small } \Gamma(H \rightarrow b\bar{b}) \text{ scenario : } r_{b\bar{b}} < 1 \text{ and } r_{gg} \cdot r_{\gamma\gamma} \sim 1 \quad (3.9b)$$

The light stau scenario can be realized for the H boson whose weak boson couplings are SM-like (nearly maximal) when a light stau loop interfere constructively to the W boson loop contribution to the $H \rightarrow \gamma\gamma$ amplitude, just as in the decoupling scenario [12, 19].

The small $\Gamma(H \rightarrow b\bar{b})$ scenario can be realized when the b-quark mass receives large radiative corrections which grows with $\mu \tan \beta$ [30].

Because the two scenarios have distinct predictions for R_{ZZ} and $R_{\tau\bar{\tau}}$, which can be tested in the current run of the LHC, we explore their consequences carefully in the extended parameter space of the MSSM.

For definiteness, we explore the following MSSM parameter regions,

$$\begin{aligned} 5 &\leq \tan \beta \leq 40, \quad 110 \leq M_{H^\pm} \leq 210, \\ 1000 \text{ GeV} &\leq A_t \leq 3600 \text{ GeV}, \quad 500 \text{ GeV} \leq \mu \leq 2000 \text{ GeV}, \\ 300 \text{ GeV} &\leq M_Q = M_U = M_D \leq 1500 \text{ GeV}. \end{aligned} \quad (3.10)$$

The following parameters are set to fixed values,

$$\begin{aligned} A_b &= A_\tau = 1 \text{ TeV}, \\ M_3 &= 800 \text{ GeV}, \quad M_2 = 200 \text{ GeV}, \quad M_1 = 100 \text{ GeV}, \end{aligned} \quad (3.11)$$

since they do not affect significantly the property of the Higgs bosons. The slepton soft mass parameters are explored in the region

$$50 \text{ GeV} \leq M_L = M_E \leq 500 \text{ GeV} \quad (3.12)$$

for the light stau scenario, while it is set to a fixed value

$$M_L = M_E = 1 \text{ TeV} \quad (3.13)$$

for the small $\Gamma(H \rightarrow b\bar{b})$ scenario.

3.1 Light stau scenario

3.1.1 $R_{\gamma\gamma}$

In this section, we examine $R_{\gamma\gamma}$, R_{ZZ} and $R_{\tau\bar{\tau}}$ in the light stau scenario where the mass of the heavier CP even Higgs boson is $125 \pm 2 \text{ GeV}$ and a large $R_{\gamma\gamma}$ is obtained by increasing $r_{\gamma\gamma}$ eq.(3.9a).

Light sfermions in the third generation can have important contribution to $r_{\gamma\gamma}$. When the Higgs coupling to $\tilde{f}_L\tilde{f}_R$ is large, the lighter sfermion loop adds constructively to the main W boson loop contribution to the $H \rightarrow \gamma\gamma$ amplitude, whereas the heavier sfermion adds destructively. Hence, the larger the mass splitting of sfermions is, the larger the enhancement of $r_{\gamma\gamma}$ should be. However, when a squark contribute constructively to $r_{\gamma\gamma}$, it contributes more destructively to r_{gg} where the dominant contribution is from the top quark loop. Accordingly, the enhancement of $r_{\gamma\gamma}$ due e.g. to the stop loop can be compensated by the stronger suppression of r_{gg} , resulting in smaller $R_{\gamma\gamma}$ [31]. The Higgs coupling to left and right handed stops is written as [32]

$$g_{H\tilde{t}_L\tilde{t}_R} = -\frac{M_t}{2} \left(\frac{\mu}{\tan\beta} - A_t \right). \quad (3.14)$$

As we have discussed in Section 2, in order for H to acquire a mass as large as 125 GeV, large A_t may be necessary, and the Higgs coupling eq.(3.14) can be large. Hence, a light stop generally lead to

$$r_{gg} < 1, \quad r_{\gamma\gamma} > 1, \quad (3.15)$$

whereas

$$r_{gg} \cdot r_{\gamma\gamma} < 1, \quad (3.16)$$

because the suppression rate in r_{gg} is larger than the enhancement rate in $r_{\gamma\gamma}$. Light slepton in the third generation, stau, with the large Higgs coupling to $\tilde{\tau}_L\tilde{\tau}_R$ can increase $r_{\gamma\gamma}$ without decreasing r_{gg} . Hence, with light stau and heavy squarks, we can expect

$$r_{gg} \cdot r_{\gamma\gamma} > 1. \quad (3.17)$$

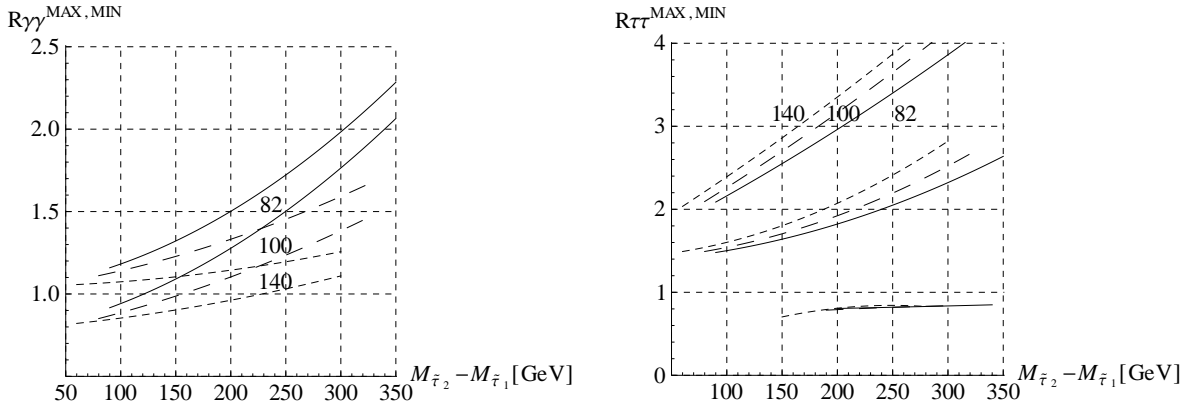


Figure 1. (Left) The maximum and minimum values of $R_{\gamma\gamma}$ are plotted against the mass difference between the lighter and heavier staus, for three different values of the lighter stau mass, 82 GeV (solid line), 100 GeV (dashed line) and 140 GeV (dotted line) in the light stau scenario. The maximum value of $R_{\gamma\gamma}$ is achieved for heavy stops, since light stop tends to decrease $R_{\gamma\gamma}$ as in eq.(3.16). (Right) The maximum and minimum values of $R_{\tau\tau}$ against the mass difference between the lighter and heavier staus, for three different values of the lighter stau mass, 82 GeV (solid line), 100 GeV (dashed line) and 140 GeV (dotted line) in the light stau scenario. The region of enhanced $R_{\tau\tau}$ corresponds to the case (I), whereas the upper and lower values degenerated around $R_{\tau\tau} \sim 0.8$ for the case (II); see text.

The Higgs coupling to $\tilde{\tau}_L \tilde{\tau}_R$ and mass splitting in the stau mass eigenstates are correlated with each other, and they can both be large when the product of $\tan\beta$ and the Higgsino mass parameter, μ , is large [32],

$$g_{H\tilde{\tau}_L\tilde{\tau}_R} = -\frac{M_\tau}{2} (\mu \tan\beta - A_\tau), \quad (3.18)$$

$$M_{\tilde{\tau}_2}^2 - M_{\tilde{\tau}_1}^2 \simeq 2M_\tau |A_\tau - \mu \tan\beta|. \quad (3.19)$$

In Figure 1 (left), we show the maximum and minimum values of $R_{\gamma\gamma}$ as functions of the mass difference between the lighter and heavier staus, for three different values of the lighter stau mass, 82 GeV (solid line), 100 GeV (dashed line) and 140 GeV (dotted line). Here we impose in the light stau scenario the condition

$$r_{b\bar{b}} = 1, \quad (3.20)$$

so that the enhancement in the $\gamma\gamma$ production rate $R_{\gamma\gamma}$ is solely due to the light stau contribution to the $H \rightarrow \gamma\gamma$, $r_{\gamma\gamma}$. Figure 1 (left) shows that light stau increases $R_{\gamma\gamma}$, and the larger the mass splitting of staus is, the larger the enhancement of $R_{\gamma\gamma}$ becomes. The maximum value of $R_{\gamma\gamma}$ can be achieved for heavy stops, since light stop tends to decrease

$r_{gg} \cdot r_{\gamma\gamma}$, and hence $R_{\gamma\gamma}$ as in eq.(3.16).

3.1.2 R_{ZZ}

Next we consider R_{ZZ} in the light stau scenario. Even with the help of the light stau contribution, significant enhancement of $R_{\gamma\gamma}$ over unity is possible only when the heavier CP even Higgs boson H has the SM like coupling to the weak bosons as explained in the section 2. We therefore expect $R_{ZZ} \sim 1$ in this scenario. Because the HWW and HZZ couplings become strongest in the SM Higgs boson limit, $r_{ZZ} < 1$ always holds. In the limit of $r_{b\bar{b}} \sim 1$ and $r_{gg} \sim 1$, the ZZ production rate should be around unity. In our numerical scan, R_{ZZ} is found to lie between 0.8 and 1.

3.1.3 $R_{\tau\bar{\tau}}$

Here we discuss $R_{\tau\bar{\tau}}$ in the light stau scenario. The enhancement of $R_{\gamma\gamma}$ due to the lighter stau can be obtained by large values of the product of $\tan\beta$ and μ as in eqs.(3.18, 3.19). When $\mu \tan\beta$ is large, the radiative SUSY correction in the b-quark and tau lepton masses can be important,

$$M_b = \frac{Y_b}{\sqrt{2}} v \cos\beta (1 + \Delta_b), \quad (3.21)$$

$$M_\tau = \frac{Y_\tau}{\sqrt{2}} v \cos\beta (1 + \Delta_\tau), \quad (3.22)$$

where [30]

$$\Delta_b = \mu \tan\beta \left[\frac{2\alpha_s}{3\pi} M_3 I(M_{\tilde{b}_1}, M_{\tilde{b}_2}, M_3) + \frac{Y_t^2}{16\pi^2} A_t I(M_{\tilde{t}_1}, M_{\tilde{t}_2}, \mu) \right], \quad (3.23)$$

$$\Delta_\tau = \mu \tan\beta \left[\frac{g_1^2}{16\pi^2} M_1 I(M_{\tilde{\tau}_1}, M_{\tilde{\tau}_2}, M_1) + \frac{g_2^2}{16\pi^2} M_2 I(M_{\tilde{\nu}_\tau}, M_2, \mu) \right]. \quad (3.24)$$

The function $I(a, b, c)$ is given by

$$I(a, b, c) = \frac{a^2 b^2 \ln(a^2/b^2) + b^2 c^2 \ln(b^2/c^2) + c^2 a^2 \ln(c^2/a^2)}{(a^2 - b^2)(b^2 - c^2)(a^2 - c^2)}, \quad (3.25)$$

which is positive for all real a, b, c . The effective Higgs couplings to $b\bar{b}$ and $\tau\bar{\tau}$ normalized to the SM values are [33]

$$g_{Hb\bar{b}} = \frac{\cos\alpha}{\cos\beta} \left[1 - \frac{\Delta_b}{1 + \Delta_b} \left(1 - \frac{\tan\alpha}{\tan\beta} \right) \right], \quad (3.26)$$

$$g_{H\tau\bar{\tau}} = \frac{\cos\alpha}{\cos\beta} \left[1 - \frac{\Delta_\tau}{1 + \Delta_\tau} \left(1 - \frac{\tan\alpha}{\tan\beta} \right) \right], \quad (3.27)$$

and their squared values should approximately correspond to $r_{b\bar{b}}$ and $r_{\tau\bar{\tau}}$, respectively. The behavior of these couplings strongly depends on the regions of the mixing angle α , $\frac{\pi}{2} < \alpha < \frac{3}{4}\pi$ or $\frac{\pi}{4} < \alpha < \frac{\pi}{2}$ in eqs.(2.16a, 2.16b). Below we discuss $R_{\tau\bar{\tau}}$ for each case.

Case (I) for $M_{ud}^2 < 0$ and $\cos \alpha < 0$ as in eq.(2.16a) :

Since H is the SM-like Higgs boson, we can estimate its deviation from the SM limit with a small parameter ϵ as,

$$\frac{-\tan \alpha}{\tan \beta} = 1 - \epsilon, \quad (3.28)$$

in the region of eq.(2.16a). Eq.(3.26) can then be expressed as

$$g_{Hb\bar{b}} = 1 + \epsilon - \frac{\Delta_b}{1 + \Delta_b}(2 + \epsilon) + O(\epsilon^2), \quad (3.29)$$

while eq.(3.27) may be expressed as

$$g_{H\tau\bar{\tau}} = 1 + \epsilon + O(\epsilon^2), \quad (3.30)$$

since Δ_τ is significantly smaller than Δ_b due to the electroweak couplings as in eq.(3.24). From these ratio of couplings, $(r_{b\bar{b}})^{-1} \cdot r_{\tau\bar{\tau}}$ in eq.(3.7c) is calculated and we find

$$R_{\tau\bar{\tau}} \simeq r_{gg} \cdot \left(1 + (2 - \epsilon) \frac{\Delta_b}{1 + \Delta_b}\right)^2. \quad (3.31)$$

$R_{\tau\bar{\tau}}$ should be always larger than unity if Δ_b is positive and $r_{gg} \sim 1$. Note that Δ_b is positive in the MSSM parameter region we explore.

Our assumption of $r_{b\bar{b}} = 1$ in eq.(3.20) can be satisfied with $\epsilon = 2\Delta_b$, which leads to

$$R_{\tau\bar{\tau}} \simeq r_{gg} \cdot \left(1 + 2\Delta_b \frac{1 - \Delta_b}{1 + \Delta_b}\right)^2. \quad (3.32)$$

Case (II) for $M_{ud}^2 > 0$ and $\cos \alpha > 0$ as in eq.(2.16b) :

In this region we can express $\tan \alpha / \tan \beta$ (> 0) with small ϵ as

$$\frac{\tan \alpha}{\tan \beta} = 1 - \epsilon. \quad (3.33)$$

Eq.(3.26) can now be expressed as

$$g_{Hb\bar{b}} = 1 + \left(1 - \frac{\Delta_b}{1 + \Delta_b}\right) \epsilon + O(\epsilon^2), \quad (3.34)$$

while eq.(3.27) may be expressed as

$$g_{H\tau\bar{\tau}} = 1 + \epsilon + O(\epsilon^2), \quad (3.35)$$

for the same reason as above. We then find

$$R_{\tau\bar{\tau}} \simeq r_{gg} \cdot \left(1 + \epsilon \frac{\Delta_b}{1 + \Delta_b}\right). \quad (3.36)$$

Our assumption of $\gamma_{b\bar{b}} = 1$ in eq.(3.20) implies with $\epsilon \approx 0$, which gives

$$R_{\tau\bar{\tau}} \simeq r_{gg}. \quad (3.37)$$

We therefore expect little dependence of $R_{\tau\bar{\tau}}$ on the stau parameters in this region.

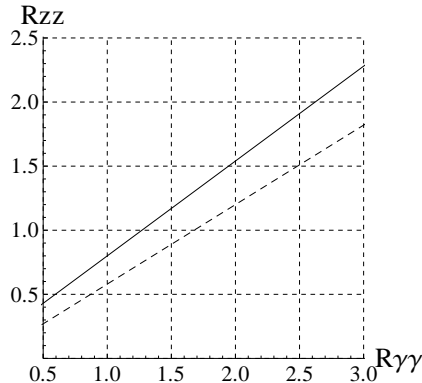


Figure 2. Correlation between $R_{\gamma\gamma}$ and R_{ZZ} with the maximum value of R_{ZZ} (solid line) and the minimum value of R_{ZZ} (dashed line) in the small $\Gamma(H \rightarrow b\bar{b})$ scenario. The maximization of R_{ZZ} is obtained for heavy stops, while the minimization of R_{ZZ} is obtained for light stops.

Results for both cases are shown in Figure 1 (right), which shows the maximum and minimum values of $R_{\tau\bar{\tau}}$ as functions of the mass difference between the lighter and heavier staus, for three different values of the lighter stau mass, 82 GeV (solid line), 100 GeV (dashed line) and 140 GeV (dotted line) in the light stau scenario.

The enhanced $R_{\tau\bar{\tau}} (> 1)$ regions are found for the case (I). Both large mass splittings and large Δ_b can be obtained for large $\mu \tan \beta$ as in eqs.(3.19, 3.23). Hence the enhancement of $R_{\tau\bar{\tau}}$ for the large stau mass splitting can be understood by the approximation eq.(3.32).

On the other hand, in the region (II), we find $R_{\tau\bar{\tau}} \sim 0.8$ almost independent of the stau mass difference and the lighter stau mass. The maximum and minimum values are almost degenerated and cannot be distinguished in the plot. It depends neither on $\Delta M_{\bar{\tau}}$ nor on the lighter stau mass as is expected from the approximate result of eq.(3.37).

Therefore, when $R_{\gamma\gamma}$ is enhanced by a light stau contribution, $R_{\tau\bar{\tau}}$ can be either significantly enhanced or slightly smaller than unity in the light stau scenario.

3.2 Small $\Gamma(H \rightarrow b\bar{b})$ scenario

3.2.1 $R_{\gamma\gamma}$ and R_{ZZ}

If the stau masses are around 1 TeV as in eq.(3.12), their contribution to the $\gamma\gamma$ rate is suppressed, and the only alternative way to enhance $R_{\gamma\gamma}$ in eq.(3.7a) is to suppress $\Gamma(H \rightarrow b\bar{b})$ as,

$$(r_{b\bar{b}})^{-1} > 1 \quad (3.38)$$

In this section, we examine the small $\Gamma(H \rightarrow b\bar{b})$ scenario where the mass of the heavier CP even Higgs boson is 125 ± 2 GeV and enhancement of the two photon production rate is obtained by the suppressed $r_{b\bar{b}}$ eq.(3.9b).

When eq.(3.38) is satisfied, not only $R_{\gamma\gamma}$ but also R_{ZZ} should be enhanced. Figure 2 shows the correlation between $R_{\gamma\gamma}$ and R_{ZZ} , with the maximum value of R_{ZZ} (solid line) and the minimum value of R_{ZZ} (dashed line). The maximum of R_{ZZ} is obtained for heavy stops, while the minimum of R_{ZZ} is obtained for light stops. We find that R_{ZZ} is always

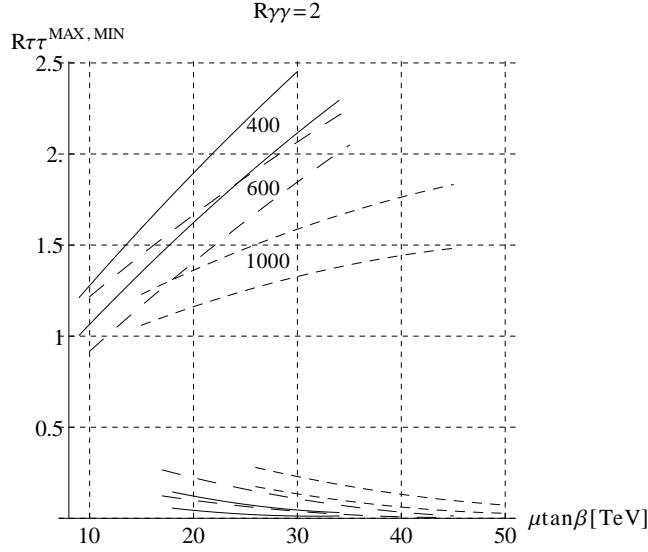


Figure 3. The maximum and minimum values of $R_{\tau\bar{\tau}}$ as functions of the product of μ and $\tan\beta$, for three different values of the lighter stop mass, 400 GeV (solid line), 600 GeV (dashed line) and 1000 GeV (dotted line) in the small $\Gamma(H \rightarrow b\bar{b})$ scenario. The enhancement of $R_{\gamma\gamma}$ is obtained due to the suppression of $r_{b\bar{b}}$ and $R_{\gamma\gamma}$ is now set to 2.

smaller than $R_{\gamma\gamma}$. This is simply because $R_{\gamma\gamma}/R_{ZZ} = r_{\gamma\gamma}/r_{ZZ}$, where $r_{\gamma\gamma}$ can be enhanced by the stop contribution while r_{ZZ} can never exceed 1.

3.2.2 $R_{\tau\bar{\tau}}$

Here we consider $R_{\tau\bar{\tau}}$ in the small $\Gamma(H \rightarrow b\bar{b})$ scenario, again for the case (I) eq.(2.16a) and the case (II) eq.(2.16b).

Case (I) for $M_{ud}^2 < 0$ and $\cos\alpha < 0$ as in eq.(2.16a) :

From the Higgs effective coupling to $b\bar{b}$ in eq.(3.29), the small $\Gamma(H \rightarrow b\bar{b})$ scenario, $0 < \gamma_{b\bar{b}} < 1$, can be obtained when

$$\Delta_b - 1 < \epsilon < 2\Delta_b, \quad (3.39)$$

which gives, from eq.(3.31),

$$r_{gg} \left(1 + (3 - \Delta_b) \frac{\Delta_b}{1 + \Delta_b} \right)^2 > R_{\tau\bar{\tau}} > r_{gg} \left(1 + 2\Delta_b \frac{1 - \Delta_b}{1 + \Delta_b} \right)^2. \quad (3.40)$$

This means that $R_{\tau\bar{\tau}}$ can be enhanced as $r_{b\bar{b}}$ becomes small, if r_{gg} is around 1.

Case (II) for $M_{ud}^2 > 0$ and $\cos\alpha > 0$ as in eq.(2.16b) :

From eq.(3.34), the small $\Gamma(H \rightarrow b\bar{b})$, $r_{b\bar{b}} < 1$, can be obtained when $\epsilon < 0$, and we find from eq.(3.36),

$$R_{\tau\bar{\tau}} < r_{gg}. \quad (3.41)$$

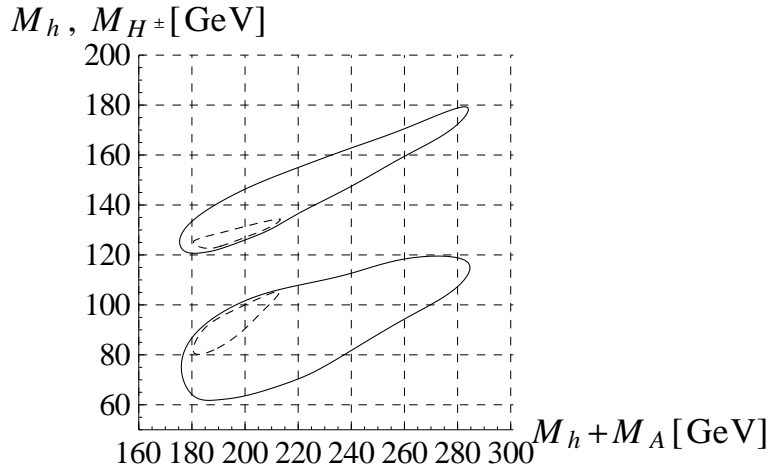


Figure 4. Allowed mass regions with $R_{\gamma\gamma} = 2.0 \pm 0.5$ in the M_h and $M_h + M_A$ space (lower plots) and in the M_{H^\pm} and $M_h + M_A$ space (upper plots), for the light stau scenario (dashed line) and the small $\Gamma(H \rightarrow b\bar{b})$ scenario (solid line).

This means that $R_{\tau\bar{\tau}}$ can be suppressed in this region as $r_{b\bar{b}}$ becomes small.

We show in Figure 3 the maximum and minimum values of $R_{\tau\bar{\tau}}$ as functions of the product of μ and $\tan\beta$, for three different values of the lighter stop mass, 400 GeV (solid line), 600 GeV (dashed line) and 1000 GeV (dotted line). The enhancement of $R_{\gamma\gamma}$ is obtained due to the suppression of $r_{b\bar{b}}$ and $R_{\gamma\gamma}$ is now set to 2.

The enhanced $R_{\tau\bar{\tau}} (\gtrsim 1)$ regions are found for the case (I). The enhancement with $\mu \tan\beta$ comes from Δ_b in eq.(3.31). The plot shows that as stops become light, $R_{\tau\bar{\tau}}$ can be larger. This tendency follows from eqs.(3.39, 3.40). Since the light stops decrease $r_{gg} \cdot r_{\gamma\gamma}$, the constraint $R_{\gamma\gamma} = r_{gg} \cdot r_{\gamma\gamma} (r_{b\bar{b}})^{-1} = 2$ implies that $r_{b\bar{b}}$ should be suppressed stronger for lighter stops. The more suppressed $(r_{b\bar{b}})^{-1}$ leads to the more enhanced $R_{\tau\bar{\tau}}$, as we can see in eqs.(3.39, 3.40).

The region of small $R_{\tau\bar{\tau}} (< 1)$ is predicted for the case (II). The plot shows that $R_{\tau\bar{\tau}}$ decreases as $\mu \tan\beta$ grows, as expected from eq.(3.36), since now $\epsilon < 0$. In contrast to the case (I), $R_{\tau\bar{\tau}}$ becomes small as the lighter stop becomes light. This follows from eq.(3.41).

4 Constraints on the other Higgs bosons

In contrast to the decoupling scenarios of the MSSM, in our two scenarios where the heavier of the CP even Higgs bosons has a mass around 125 GeV, and at the same time, has the SM-like (nearly maximum) coupling to the weak bosons, none of the other Higgs bosons can be very heavy. The masses of the CP odd and charged Higgs bosons are bounded from above when H is a SM-like Higgs boson, as explained in Section 2; see eqs.(2.13, 2.14). From eq.(2.14), the largest M_A may be obtained when

$$\bar{A}_t^2 = 6 + \frac{\bar{\mu}^2}{2}, \quad (4.1)$$

whereas in order to obtain M_H as large as 125 GeV, $\bar{A}_t^2 \sim 6$ is necessary from eqs.(2.7a, 2.11b).

Figure 4 shows the mass regions with $R_{\gamma\gamma} = 2.0 \pm 0.5$ in the M_h and $M_h + M_A$ space (lower plots) and in the M_{H^\pm} and $M_h + M_A$ space (upper plots), for the light stau scenario (dashed line) and the small $\Gamma(H \rightarrow b\bar{b})$ scenario (solid line). The mass region with large M_A and M_H^\pm are obtained by the large radiative SUSY correction in eq.(2.14). The lower bound on M_h comes from the upper bound on the cross section $\sigma(e^+e^- \rightarrow Zh)$, and the lower bound on $M_h + M_A$ comes from the upper bound on $\sigma(e^+e^- \rightarrow Ah)$. The reason for large difference of these two scenario is because $r_{b\bar{b}}$ is constrained to be 1 in the light stau scenario, while it is not constrained in the small $\Gamma(H \rightarrow b\bar{b})$ scenario. Since h is non SM-like Higgs boson in our scenarios, the cross section $\sigma(e^+e^- \rightarrow Zh)$ is highly suppressed, while the cross sections $\sigma(e^+e^- \rightarrow ZH)$ ($\sqrt{s} \simeq 215$ GeV) and $\sigma(e^+e^- \rightarrow Ah)$ ($180 \lesssim \sqrt{s} \lesssim 280$ GeV) will not be suppressed. Hence these Higgs bosons should be discovered in the future e^+e^- collider. The charge Higgs boson with $M_{H^\pm} \lesssim 160$ GeV can be discovered from the top quark decay at the LHC, while with $160 \lesssim M_{H^\pm} \lesssim 180$ GeV a e^+e^- collider which can produce top quark pairs ($\sqrt{s} \sim 400$ GeV) may be necessary for its pair production.

5 Conclusion

In this study, we identify the 125 GeV state as the heavier of CP even Higgs boson in the MSSM, and study two scenarios where the two photon production rate can be larger than the SM prediction. In the light stau, the large two photon rate $R_{\gamma\gamma}$ is obtained by a light stau contribution. We find that $R_{\gamma\gamma}$ as large as 2 may be obtained with a light stau near the current mass bound, and that R_{ZZ} is slightly smaller than 1 in this scenario. Additionally we examine non-trivial enhancement of $R_{\tau\bar{\tau}}$. Due to the large radiative SUSY correction to the b-quark mass, large $R_{\tau\bar{\tau}}$ can be obtained, while as large as the SM value is also possible.

In the small $\Gamma(H \rightarrow b\bar{b})$ scenario, the large two photon rate $R_{\gamma\gamma}$ is obtained by the suppressed Higgs coupling to b-quark. Differently from the light stau scenario, not only $R_{\gamma\gamma}$ but also R_{ZZ} can be enhanced at the same time. $R_{\tau\bar{\tau}}$ can again be either largely enhanced or suppressed.

We also study mass spectrum of other three Higgs bosons, h , A and H^\pm . We discuss the maximization of M_A due to the radiative SUSY correction, when M_H is the SM-like Higgs boson. We find that both scenarios with our scanned parameter regions predict single and pair production of all the Higgs bosons in e^+e^- collisions at $\sqrt{s} \lesssim 400$ GeV. The charged Higgs boson with $120 \lesssim M_{H^\pm} \lesssim 160$ GeV may be discovered from the top quark decay at the LHC.

Acknowledgments

J.N. thanks Yoshitaro Takaesu for his help. We are thankful that the simulation in this study was executed on the Central Computing System of High Energy Accelerator Research Organization. The work of JSL was supported in part by the National Science Council of

Taiwan under Grant No. 100-2112-M-007-023-MY3. This work is also supported in part by Grant-in-Aid for scientific research (#20340064 and #23104006) from Japan Society for the Promotion of Science.

References

- [1] ATLAS Collaboration. ‘Combined search for the Standard Model Higgs boson using up to 4.9 fb^{-1} of pp collision data at $\sqrt{s} = 7 \text{ TeV}$ with the ATLAS detector at the LHC’, *Physics Letters B* 710 (2012) 49-66.
- [2] CMS Collaboration. ‘Combined results of searches for the standard model Higgs boson in pp collisions at $\sqrt{s} = 7 \text{ TeV}$ ’, arXiv:1202.1488 [hep-ex].
- [3] Stephen P. Martin. ‘A Supersymmetry Primer’, arXiv:hep-ph/9709356v6.
- [4] M. Spira, A. Djouadi, D. Graudenz, R.M. Zerwas. ‘Higgs boson production at the LHC’, *Nuclear Physics B* 453 (1995) 17-82.
- [5] G. Kane, P. Kumar, R. Lu, B. Zheng. ‘Higgs Mass Prediction for Realistic String/M Theory Vacua’, *Phys.Rev. D*85 (2012) 075026. arXiv:1112.1059 [hep-ph]
- [6] L. J. Hall, D. Pinner, J. T. Ruderman. ‘A Natural SUSY Higgs Near 125 GeV’, arXiv:1112.2703 [hep-ph]
- [7] H. Baer, V. Barger, A. Mustafayev. ‘Implications of a 125 GeV Higgs scalar for LHC SUSY and neutralino dark matter searches’, *Phys. Rev. D*85 (2012) 075010. arXiv:1112.3017 [hep-ph]
- [8] J. L. Feng, K. T. Matchev, D. Sanford. ‘Focus Point Supersymmetry Redux’, *Phys.Rev. D*85 (2012) 075007. arXiv:1112.3021 [hep-ph]
- [9] S. Heinemeyer, O. Stal, G. Weiglein. ‘Interpreting the LHC Higgs Search Results in the MSSM’, *Phys. Lett. B* 710 (2012) 201. arXiv:1112.3026v3 [hep-ph]
- [10] A. Arbey, M. Battaglia, A. Djouadi, F. Mahmoudi and J. Quevillon. ‘Implications of a 125 GeV Higgs for supersymmetric models’, *Phys.Lett. B* 708 (2012) 162-169. arXiv:1112.3028 [hep-ph]
- [11] P. Draper, P. Meade, M. Reece, D. Shih. ‘Implications of a 125 GeV Higgs for the MSSM and Low-Scale SUSY Breaking’, arXiv:1112.3068 [hep-ph]
- [12] M. Carena, S. Gori, N. R. Shah and C. E. M. Wagner. ‘A 125 GeV SM-like Higgs in the MSSM and the $\gamma\gamma$ rate’, *JHEP* 1203, 014 (2012), arXiv:1112.3336 [hep-ph]
- [13] S. Akula, B. Altunkaynak, D. Feldman, P. Nath, G. Peim. ‘Higgs Boson Mass Predictions in SUGRA Unification, Recent LHC-7 Results, and Dark Matter’, *Phys.Rev.D*85:075001,2012. arXiv:1112.3645 [hep-ph]
- [14] J. Cao, Z. Heng, J. M. Yang, Y. Zhang, J. Zhu. ‘A SM-like Higgs near 125 GeV in low energy SUSY: a comparative study for MSSM and NMSSM’, *JHEP* 1203 (2012) 086, arXiv:1202.5821v2 [hep-ph]
- [15] N. Desai, B. Mukhopadhyaya, S. Niyogi. ‘Constraints on invisible Higgs decay in MSSM in the light of diphoton rates from the LHC’, arXiv:1202.5190v1 [hep-ph]
- [16] N. Christensen, T. Han, S. Su. ‘MSSM Higgs Bosons at The LHC’, arXiv:1203.3207v1 [hep-ph]

- [17] F. Brummer, S. Kraml, S. Kulkarni. ‘Anatomy of maximal stop mixing in the MSSM’, arXiv:1204.5977v2 [hep-ph].
- [18] J. L. Feng, D. Sanford. ‘A Natural 125 GeV Higgs Boson in the MSSM from Focus Point Supersymmetry with A-Terms’, arXiv:1205.2372v1 [hep-ph].
- [19] M. Carena, S. Gori, N. R. Shah, C. E. M. Wagner and L. Wang. ‘Light Stau Phenomenology and the Higgs $\gamma\gamma$ Rate’, arXiv:1205.5842 [hep-ph]
- [20] M. Carena, J.R. Espinosa, M. Quiros and C.E.M. Wagner. ‘Analytical expressions for radiatively corrected Higgs masses and couplings in the MSSM’, Physics Letters B 355(1995) 209-221.
M. Carena, M. Quiros, C.E.M. Wagner. ‘Effective potential methods and the Higgs mass spectrum in the MSSM’, Nuclear Physics B 461 (1996) 407-436.
- [21] D. Graudenz, M. Spira, and P. Zerwas. ‘QCD corrections to Higgs boson production at proton proton colliders’, Phys. Rev. Lett. 70 (1993) 13721375
- [22] M. Ciccolini, A. Denner, S. Dittmaier. ‘Strong and electroweak corrections to the production of Higgs + 2jets via weak interactions at the LHC’, Phys. Rev. Lett. 99 (2007) 161803, arXiv:0707.0381[hep-ph]
M.Ciccolini, A.Denner and S.Dittmaier. ‘Electroweak and QCD corrections to Higgs production via vector-boson fusion at the LHC’, Phys.Rev.D77:013002,2008 arXiv:0710.4749 [hep-ph]
- [23] R. V. Harlander and W. B. Kilgore. ‘Higgs boson production in bottom quark fusion at next-to-next-to leading order’, Phys. Rev. D68 (2003) 013001, arXiv:hep-ph/0304035 [hep-ph].
- [24] J.S. Lee, A. Pilaftsis, M. Carena, S.Y. Choi, M. Drees, J. Ellis, C.E.M. Wagner. ‘CPsuperH: a Computational Tool for Higgs Phenomenology in the Minimal Supersymmetric Standard Model with Explicit CP Violation’, Comput. Phys. Commun. 156 (2004) 283317, arXiv:hep-ph/0307377.
J.S. Lee, M. Carena, J. Ellis, A. Pilaftsis, C.E.M. Wagner. ‘CPsuperH2.0: an Improved Computational Tool for Higgs Phenomenology in the MSSM with Explicit CP Violation’, Comput. Phys. Commun. 180 (2009) 312331, arXiv:0712.2360 [hep-ph].
J.S. Lee *et al.*, ‘CPsuperH2.3: an Updated Tool for Phenomenology in the MSSM with Explicit CP Violation’, work in preparation
- [25] A. Djouadi, J. Kalinowski and M. Spira. ‘HDECAY: A program for Higgs boson decays in the standard model and its supersymmetric extension’, Comput. Phys. Commun. 108 (1998) 5674, arXiv:hep-ph/9704448.
- [26] K. Nakamura *et al* (Particle Data Group). ‘Review of Particle Physics’, 2010 J. Phys. G: Nucl. Part. Phys. 37 075021.
- [27] ALEPH, DELPHI, L3, OPAL Collaborations (The LEP Working Group ”for Higgs Boson Searches”). ‘Search for Neutral MSSM Higgs Bosons at LEP’, Eur.Phys.J.C47:547-587,2006. arXiv:hep-ex/0602042v1
- [28] CMS Collaboration. ‘Search for neutral Higgs bosons decaying to tau pairs in pp collisions at $\sqrt{s} = 7$ TeV’, arXiv:1202.4083 [hep-ex]
- [29] CMS Collaboration, ‘Search for a light charged Higgs boson in top quark decays in pp collisions at $\sqrt{s} = 7$ TeV’, arXiv:1205.5736 [hep-ex]

- [30] L. Hall, R. Rattazzi and U. Sarid. ‘Top quark mass in supersymmetric SO(10) unification’, *Phys. Rev. D* 50, 70487065 (1994).
M. Carena, M. Olechowski, S. Pokorski and C.E.M. Wagner. ‘Electroweak symmetry breaking and bottom-top Yukawa unification’, *Nuclear Physics B* 426 (1994) 269-300.
D. Pierce, J. Bagger, K. Matchev and R. Zhang. ‘Precision corrections in the minimal supersymmetric standard model’, *Nuclear Physics B* 491 (1997) 3-67.
- [31] Abdelhak Djouadi. ‘Squark effects on Higgs boson production and decay at the LHC’, *Physics Letters B* 435 (1998) 101-108.
- [32] A. Djouadi, J. Kalinowski, P. Ohmann, P.M. Zerwas. ‘Heavy SUSY Higgs Bosons at e^+e^- Linear Colliders’, *Z. Phys. C* 74 (1997) 93, hep-ph/9605339.
Margarete Muhlleitner, Michael Spira. ‘Higgs boson production via gluon fusion: Squark loops at NLO QCD’, *Nuclear Physics B* 790 (2008) 1-27.
- [33] M. Carena, S. Mrenna and C. E. M. Wagner. ‘MSSM Higgs boson phenomenology at the Fermilab Tevatron collider’, *Phys. Rev. D* 60, 075010 (1999).
M. Carena, S. Mrenna and C. E. M. Wagner. ‘Complementarity of the CERN LEP collider, the Fermilab Tevatron, and the CERN LHC in the search for a light MSSM Higgs boson’, *Phys. Rev. D* 62, 055008 (2000).